Materials Research Proceedings 31 (2023) 634-645 https://doi.org/10.21741/9781644902592-65

# Passive vibration damping of a plate interacting with a flowing fluid using shunted piezoelectric element

Sergey Lekomtsev[a *], Valerii Matveenko[b] and Alexander Senin[c]

Institute of Continuous Media Mechanics, Ural Branch of the Russian Academy of Sciences, 1, Acad. Korolev street, Perm, 614013, Russian Federation

[a]lekomtsev@icmm.ru, [b]mvp@icmm.ru, [c]senin.a@icmm.ru

**Keywords:** Vibrations Damping, Plate, Piezoelectric Elements, Electric Circuit, Flowing Fluid, Finite Element Method

**Abstract.** This paper considers a thin plate with a single piezoceramic element located on the outer surface of the structure and connected to a series electric circuit. The dependence of complex eigenvalues of the electromechanical system on the resistance and inductance of the electric circuit is analyzed to select their optimal values for suppressing the resonant vibrations of the plate interacting with a flowing fluid. The numerical studies show that in contrast to the known analytical expression, these values lead to a smaller change in the frequency spectrum of the original system and provide more effective damping of vibrations in terms of maximum rate of vibration decay. The actual decrease in the amplitude of vibrations is demonstrated by the frequency response curves.

## Introduction

The technique of passive damping of structure vibrations by means of attaching a piezoelectric element to it and connecting its electroded surfaces to an external electric circuit with impedance has been known long enough in various fields of advanced technologies [1, 2]. At present, this approach has found wide practical application due to the possibility of controlling the dynamic behavior of objects located in hard-to-reach places, limited space or under water. By selecting the parameters for different elements of the electric circuit, one can achieve a considerable decrease in the amplitude of the resonance or an increase in the rate of damping of free vibrations [2–9]. A comprehensive review of publications devoted to passive damping is presented in works [10–12] and monograph [13]. Worthy of mention are articles [14–21], which consider the problems of passive suppression of noise produced by underwater objects or vibrations of structures interacting with a fluid. In these papers, with the exception of [20], the question of selecting optimal parameters of the electric circuit, providing the most effective damping of a given vibration mode of the structure, is not addressed directly. In most cases, such selection is performed using the analytical expressions proposed in [2]. Of the above publications, only [19] investigates a structure that interacts with a flowing fluid. This paper considers a lifting surface in the form of a plate, which is a simplified analogue to a submerged wing, stabilizer, rudder, etc. The experiments showed that the dependence of its natural frequencies on the Reynolds number is very weak. This fact led to the assumption about the immobility of the fluid and allowed using the derived formulas [2] to determine parameters of an electric *RL*-circuit connected to piezoelectric elements. Although the results obtained have demonstrated the effectiveness of the proposed method, its applicability in the case of dependence of natural frequencies of plate vibrations on the velocity of the fluid flow or in the presence of a hydrodynamic damping mechanism in the system is not so obvious. In this connection, it is important to develop an algorithm for selecting parameters of the passive electric circuit, which will provide the most effective damping of resonant vibrations of the plate interacting with a flowing fluid.

## Governing equations and finite element formulation

We consider a thin rectangular plate with $P$ piezoelectric elements attached to its upper surface and polarized in the direction of the $z$-axis. The lower surface of the structure interacts with a fluid, which flows with velocity $U$ in the direction of the $x$-axis (Fig. 1*a*). Each $k$-th piezoelectric element ($k = 1, 2, \ldots, P$) is connected through the electroded surfaces to its own electrical circuit, consisting of the series-connected resistor $R_k$ and the inductance coil $L_k$.

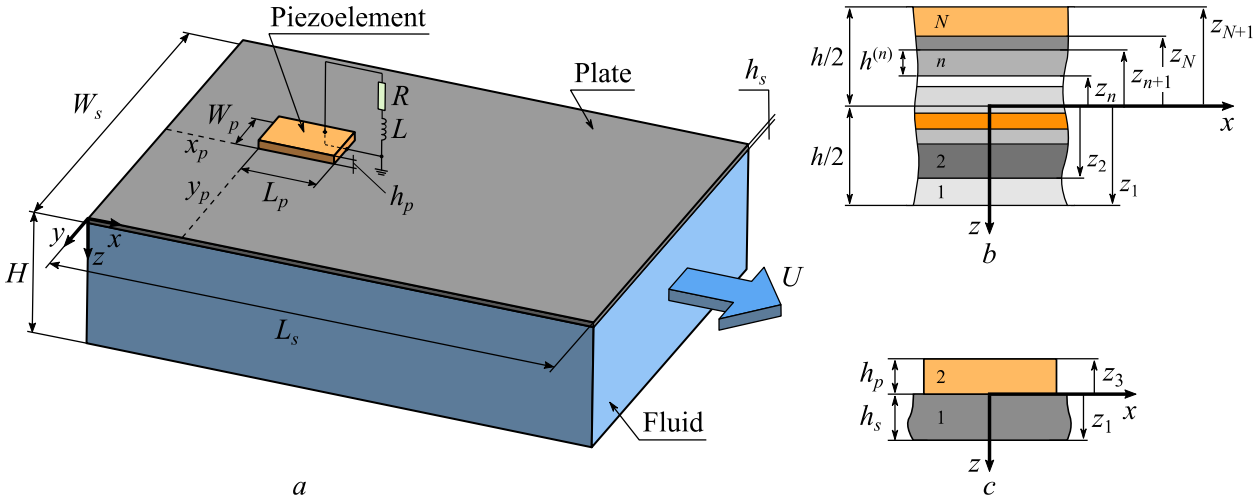


*Fig. 1. Rectangular plate with a piezoelectric element and interacting with flowing fluid*

An electroelastic body of small thickness is modeled using the classical laminated plate theory [22]. Its constitutive relations are based on the equations of the linear theory of piezoelasticity [23], which are written for the case of a plane stress state [22]. Based on the assumptions and hypotheses presented in [24], they are formulated for each $n$-th layer ($n = 1, 2, \ldots, N$) in the following form [25, 26]:

$$\begin{Bmatrix} \sigma_{xx} \\ \sigma_{yy} \\ \sigma_{xy} \end{Bmatrix}^{(n)} = \begin{bmatrix} \tilde{Q}_{11} & \tilde{Q}_{12} & 0 \\ \tilde{Q}_{21} & \tilde{Q}_{22} & 0 \\ 0 & 0 & \tilde{Q}_{66} \end{bmatrix}^{(n)} \begin{Bmatrix} \varepsilon_{xx} \\ \varepsilon_{yy} \\ \varepsilon_{xy} \end{Bmatrix} - \begin{bmatrix} 0 & 0 & \tilde{e}_{31} \\ 0 & 0 & \tilde{e}_{32} \\ 0 & 0 & 0 \end{bmatrix}^{(n)} \begin{Bmatrix} 0 \\ 0 \\ E_z \end{Bmatrix}^{(n)} \quad \text{or} \quad \boldsymbol{\sigma}^{(n)} = \tilde{\mathbf{c}}^{(n)}\boldsymbol{\varepsilon} - \tilde{\mathbf{e}}^{(n)}\mathbf{E}^{(n)}, \tag{1}$$

$$\begin{Bmatrix} 0 \\ 0 \\ D_z \end{Bmatrix}^{(n)} = \begin{bmatrix} 0 & 0 & 0 \\ 0 & 0 & 0 \\ \tilde{e}_{31} & \tilde{e}_{32} & 0 \end{bmatrix}^{(n)} \begin{Bmatrix} \varepsilon_{xx} \\ \varepsilon_{yy} \\ \varepsilon_{xy} \end{Bmatrix} + \begin{bmatrix} 0 & 0 & 0 \\ 0 & 0 & 0 \\ 0 & 0 & \tilde{\delta}_{33} \end{bmatrix}^{(n)} \begin{Bmatrix} 0 \\ 0 \\ E_z \end{Bmatrix}^{(n)} \quad \text{or} \quad \mathbf{D}^{(n)} = (\tilde{\mathbf{e}}^{(n)})^{\mathrm{T}}\boldsymbol{\varepsilon} + \tilde{\boldsymbol{\delta}}^{(n)}\mathbf{E}^{(n)}. \tag{2}$$

Here: $\boldsymbol{\sigma}$ and $\boldsymbol{\varepsilon}$ are the vectors containing components of the stress and small strain tensors; $\mathbf{E}$, $\mathbf{D}$ are the vectors of electric field intensity and electric displacements; $\tilde{\mathbf{c}}$ is the reduced stiffness matrix evaluated at a constant electric field; $\tilde{\mathbf{e}}$ is the matrix of reduced piezoelectric constants; $\tilde{\boldsymbol{\delta}}$ is the matrix of the reduced dielectric constants evaluated at a constant mechanical strain. When the piezoelectric effect in $n$-th layer is absent, the part containing matrix $\tilde{\boldsymbol{\delta}}$ should be excluded.

The elements of the matrices $\tilde{\mathbf{c}}^{(n)}$, $\tilde{\mathbf{e}}^{(n)}$ and $\tilde{\boldsymbol{\delta}}^{(n)}$ are calculated as follows [27, 28]:

$$\tilde{Q}_{ij}^{(n)} = Q_{ij}^{(n)} - \frac{Q_{i3}^{(n)}Q_{j3}^{(n)}}{Q_{33}^{(n)}}, \quad \tilde{Q}_{66}^{(n)} = Q_{66}^{(n)}, \quad \tilde{e}_{3j}^{(n)} = e_{3j}^{(n)} - \frac{e_{33}Q_{j3}^{(n)}}{Q_{33}^{(n)}}, \quad \tilde{\delta}_{33}^{(n)} = \delta_{33}^{(n)} + \frac{e_{33}^{(n)}e_{33}^{(n)}}{Q_{33}^{(n)}}, \quad i, j = \overline{1,2}. \tag{3}$$

The coefficients $Q_{ij}^{(n)}$ can be written in terms of the engineering constants of the *n*-th layer:

$$Q_{11}^{(n)}=\frac{E_1^{(n)}}{1-\nu_{12}^{(n)}\nu_{21}^{(n)}},\ Q_{12}^{(n)}=\frac{\nu_{12}^{(n)}E_2^{(n)}}{1-\nu_{12}^{(n)}\nu_{21}^{(n)}}=\frac{\nu_{21}^{(n)}E_1^{(n)}}{1-\nu_{12}^{(n)}\nu_{21}^{(n)}},\ Q_{22}^{(n)}=\frac{E_2^{(n)}}{1-\nu_{12}^{(n)}\nu_{21}^{(n)}},\ Q_{66}^{(n)}=G_{12}^{(n)}, \tag{4}$$

where $E_1$ and $E_2$ are the Young moduli of the material in the *x*- and *y*- directions, $\nu_{ij}$ are the Poisson ratios, $G_{12}$ is the shear module in the *xy* plane.

The electric field intensity vector is normal to the electrodes and its intensity in the *n*-th piezoelectric layer is uniform [24]:

$$E_z^{(n)}=-\frac{\psi^{(n)}}{h^{(n)}}, \tag{5}$$

where $\psi^{(n)}$ is the potential difference between the top and bottom electrodes of the *n*-th piezoelectric layer, $h^{(n)}$ is the thickness of the *n*-th layer.

The generalized vector $\boldsymbol{\varepsilon}$ containing middle surface strains and curvatures is written as [22]:

$$\boldsymbol{\varepsilon}=\left\{\varepsilon_{xx}^0,\varepsilon_{yy}^0,\gamma_{xy}^0,\varepsilon_{xx}^1,\varepsilon_{yy}^1,\gamma_{xy}^1,\right\}^{\mathrm{T}}=\left\{\frac{\partial u}{\partial x},\frac{\partial v}{\partial y},\frac{\partial u}{\partial y}+\frac{\partial v}{\partial x},-\frac{\partial^2 w}{\partial x^2},-\frac{\partial^2 w}{\partial y^2},-2\frac{\partial^2 w}{\partial x\partial y}\right\}^{\mathrm{T}}, \tag{6}$$

where *u*, *v*, *w* are the displacements of the points on the middle surface of the plate in the direction of the corresponding axes of the Cartesian coordinates *x*, *y*, *z*.

Using expressions (1), (5) the vector of the forces and moments **t** is defined as:

$$\mathbf{t}=\left\{N_{xx},N_{yy},N_{xy},M_{xx},M_{yy},M_{xy}\right\}^{\mathrm{T}}=\mathbf{S}\boldsymbol{\varepsilon}-\mathbf{G}\mathbf{E}_z, \tag{7}$$

$$\mathbf{S}=\begin{bmatrix}A_{11}&A_{12}&A_{16}&B_{11}&B_{12}&B_{16}\\A_{12}&A_{22}&A_{26}&B_{12}&B_{22}&B_{26}\\A_{16}&A_{26}&A_{66}&B_{16}&B_{26}&B_{66}\\B_{11}&B_{12}&B_{16}&D_{11}&D_{12}&D_{16}\\B_{12}&B_{22}&B_{26}&D_{12}&D_{22}&D_{26}\\B_{16}&B_{26}&B_{66}&D_{16}&D_{26}&D_{66}\end{bmatrix},\quad \mathbf{G}=\begin{bmatrix}g_{11}&g_{12}&\cdots&g_{1n}&\cdots&g_{1N}\\g_{21}&g_{22}&\cdots&g_{2n}&\cdots&g_{2N}\\0&0&\cdots&0&\cdots&0\\g'_{11}&g'_{12}&\cdots&g'_{1n}&\cdots&g'_{1N}\\g'_{21}&g'_{22}&\cdots&g'_{2n}&\cdots&g'_{2N}\\0&0&\cdots&0&\cdots&0\end{bmatrix},$$

where the coefficients entering into the matrices **S** and **G** are calculated as follows:

$$A_{ij}=\sum_{n=1}^{N}\tilde{Q}_{ij}^{(n)}\left(z_n-z_{n+1}\right),\ B_{ij}=\frac{1}{2}\sum_{n=1}^{N}\tilde{Q}_{ij}^{(n)}\left(z_n^2-z_{n+1}^2\right),\ C_{ij}=\frac{1}{3}\sum_{n=1}^{N}\tilde{Q}_{ij}^{(n)}\left(z_n^3-z_{n+1}^3\right),\ i=1,2,6, \tag{8}$$

$$g_{in}=\left(z_n-z_{n+1}\right)\tilde{e}_{3i}^{(n)}=h^{(n)}\tilde{e}_{3i}^{(n)},\quad g'_{in}=\frac{1}{2}\left(z_n^2-z_{n+1}^2\right)\tilde{e}_{3i}^{(n)},\quad i=1,2.$$

According to equation (5), the components $E_z$ of the electric field intensity vector **E** are determined in each *n*-th layer of the material using the following expressions:

$$\mathbf{E}_z = -\mathbf{B}_\psi \boldsymbol{\psi} = -\begin{bmatrix} 1/h^{(1)} & 0 & 0 & 0 \\ 0 & 1/h^{(2)} & 0 & 0 \\ 0 & 0 & \ddots & 0 \\ 0 & 0 & 0 & 1/h^{(N)} \end{bmatrix} \begin{Bmatrix} \psi^{(1)} \\ \psi^{(2)} \\ \vdots \\ \psi^{(N)} \end{Bmatrix}. \tag{9}$$

The equation (2) can also be rewritten taking into account (5):

$$\mathbf{D}_z = \mathbf{G}^{\mathrm{T}}\boldsymbol{\varepsilon} + \mathbf{H}\mathbf{E}_z, \quad \mathbf{H} = \operatorname{diag}\left(\tilde{\alpha}_{33}^{(1)}, \tilde{\alpha}_{33}^{(2)}, \ldots, \tilde{\alpha}_{33}^{(n)}, \ldots, \tilde{\alpha}_{33}^{(N)}\right). \tag{10}$$

The above relations allow us to describe the behavior of a monolithic composite plate, which in the general case has $N$ orthotropic elastic and piezoelectric layers (Fig. 1*b*). When modeling a structure with piezoelectric elements on its upper surface it is assumed that the host plate consists of $M$ elastic orthotropic layers, and because of the presence of the piezoelectric element one more piezoelectric layer is added to already existing ones (Fig. 1*c*). In this case, expression (7) goes to:

$$\begin{aligned} &\mathbf{T} = \mathbf{S}_s\boldsymbol{\varepsilon}, && n = \overline{1, M}, \\ &\mathbf{T} = \mathbf{S}_p\boldsymbol{\varepsilon} - \mathbf{G}\mathbf{E}_z, && n = N, \end{aligned} \tag{11}$$

and relation (10) is written only for $n = N$.

The piezoelectric element is a single layer of transversely isotropic material of thickness $h_p$, which has only two electrical unknown quantities: the potential difference $\psi$ (voltage) and the electrical charge $q$. The matrices entering into expressions (9) and (10) take the following form:

$$\mathbf{G} = \left\{g_{11}, g_{21}, 0, g'_{11}, g'_{21}, 0\right\}^{\mathrm{T}}, \quad \mathbf{B}_\psi = 1/h_p, \quad \mathbf{H} = \tilde{\alpha}_{33}, \tag{12}$$

The mathematical formulation of the dynamics problem for an electroelastic plate is based on the variational principle of virtual displacements, which is written in the matrix form taking into account the work of inertia and external surface forces [24, 29]:

$$\begin{aligned} &\sum_{k=1}^{P} \int\limits_{S_{p_k}} \left( \delta\boldsymbol{\varepsilon}^{\mathrm{T}}\mathbf{S}_{p_k}\boldsymbol{\varepsilon} + \delta\boldsymbol{\varepsilon}^{\mathrm{T}}\mathbf{G}\frac{\psi_k}{h_{p_k}} + \frac{\delta\psi_k}{h_{p_k}}\mathbf{G}^{\mathrm{T}}\boldsymbol{\varepsilon} \right) \mathrm{d}S - \delta\boldsymbol{\psi}^{\mathrm{T}}\mathbf{C}_p\boldsymbol{\psi} + \sum_{k=1}^{P} \int\limits_{S_{p_k}} \delta\mathbf{d}^{\mathrm{T}}\mathbf{J}_{p_k}\ddot{\mathbf{d}}\mathrm{d}S + \delta\boldsymbol{\psi}^{\mathrm{T}}\mathbf{q} + \\ &+ \int\limits_{S_s} \delta\boldsymbol{\varepsilon}^{\mathrm{T}}\mathbf{S}_s\boldsymbol{\varepsilon}\mathrm{d}S + \int\limits_{S_s} \delta\mathbf{d}^{\mathrm{T}}\mathbf{J}_s\ddot{\mathbf{d}}\mathrm{d}S - \int\limits_{S_f} \delta w p \mathrm{d}S = \int\limits_{S_\sigma} \delta\mathbf{d}^{\mathrm{T}}\mathbf{f}\mathrm{d}S \end{aligned} \tag{13}$$

and is supplemented by the equation for a series $RL$-circuit connecting the voltage $\psi_k$ at each piezoelectric element to the corresponding electric charge $q_k$ [24]:

$$\delta\mathbf{q}^{\mathrm{T}}\boldsymbol{\psi} - \delta\mathbf{q}^{\mathrm{T}}\mathbf{R}\dot{\mathbf{q}} - \delta\mathbf{q}^{\mathrm{T}}\mathbf{L}\ddot{\mathbf{q}} = 0. \tag{14}$$

Hereinafter, the subindexes "$s$", "$p$" and "$f$" denote the belongingness of the quantity to the structure, piezoelectric element or fluid; $\mathbf{d} = \{u, v, w, \theta_x, \theta_y\}^{\mathrm{T}}$ is the generalized vector of plate displacements, including rotation angles $\theta_x = \partial w/\partial x$ and $\theta_y = \partial w/\partial y$; $\boldsymbol{\psi} = \{\psi_1, \psi_2, \ldots, \psi_P\}^{\mathrm{T}}$ and $\mathbf{q} = \{q_1, q_2, \ldots, q_P\}^{\mathrm{T}}$ are the vectors of potential differences and electrical charges; $S_s$ is the whole plate area; $S_f$ and $S_\sigma$ are the regions of the plate, which interact with the flowing fluid and are under the static load $\mathbf{f}$, respectively; $p$ is the hydrodynamic pressure of the fluid; $\mathbf{R} = \operatorname{diag}(R_1, R_2, \ldots, R_P)$

and $\mathbf{L} = \mathrm{diag}(L_1, L_2, \ldots, L_P)$ are the diagonal matrices containing the values of resistance and inductance of the *RL*-circuits connected to each of the piezoelectric elements The matrices of the inertia **J** and capacitances $\mathbf{C}_p$ are defined using expressions:

$$\mathbf{J} = \begin{bmatrix} J_0 & 0 & 0 & -J_1 & 0 \\ 0 & J_0 & 0 & 0 & -J_1 \\ 0 & 0 & J_0 & 0 & 0 \\ -J_1 & 0 & 0 & J_2 & 0 \\ 0 & -J_1 & 0 & 0 & J_2 \end{bmatrix}, \quad \mathbf{C}_p = \begin{bmatrix} C_1 & 0 & 0 & 0 & 0 \\ 0 & C_2 & 0 & 0 & 0 \\ 0 & 0 & C_3 & 0 & 0 \\ 0 & 0 & 0 & \ddots & 0 \\ 0 & 0 & 0 & 0 & C_P \end{bmatrix}, \tag{15}$$

$$J_0 = \sum_{n=1}^{N} \rho^{(n)} \left( z_n - z_{n+1} \right), \quad J_1 = \frac{1}{2} \sum_{n=1}^{N} \rho^{(n)} \left( z_n^2 - z_{n+1}^2 \right), \quad J_2 = \frac{1}{3} \sum_{n=1}^{N} \rho^{(n)} \left( z_n^3 - z_{n+1}^3 \right), \quad C_k = \tilde{\alpha}_{33}^{(k)} A_k \big/ h_{p_k},$$

where $\rho^{(n)}$ is the density of the *n*-th layer of a composite material, $C_k$ and $A_k$ are the capacitance and the area of the *k*-th piezoelectric layer.

In the case of small perturbations the basic relations, describing the vortex-free dynamics of an ideal compressible fluid of volume $V_f$, are formulated in terms of the perturbation velocity potential $\varphi$ [30–32]. The corresponding second-order differential equation written in the Cartesian coordinate system (*x, y, z*) associated with the elastic plate is transformed together with the impermeability condition and boundary conditions to the weak form using the Bubnov – Galerkin method [32]:

$$\int_{V_f} \nabla F_m \cdot \nabla \hat{\varphi} \mathrm{d}V + \int_{V_f} F_m \frac{1}{c^2} \frac{\partial^2 \hat{\varphi}}{\partial t^2} \mathrm{d}V + \int_{V_f} F_m \frac{2U}{c^2} \frac{\partial^2 \hat{\varphi}}{\partial t \partial x} \mathrm{d}V - \int_{V_f} F_m \frac{U^2}{c^2} \frac{\partial^2 \hat{\varphi}}{\partial x^2} \mathrm{d}V - \tag{16}$$

$$- \int_{S_f} F_m \frac{\partial \hat{w}}{\partial t} \mathrm{d}S - \int_{S_f} F_m U \frac{\partial \hat{w}}{\partial x} \mathrm{d}S = 0, \quad m = \overline{1, m_f}.$$

Here: $\hat{\varphi}$ and $\hat{w}$ are the trial solutions for the velocity potential $\varphi$ and normal displacements of the plate *w*; *c* is the speed of sound in a fluid; *t* is time; $F_m$ and $m_f$ are the basis functions and their number.

The hydrodynamic pressure *p* in equation (13) is calculated using linearized Bernoulli's formula

$$p = -\rho_f \left( \frac{\partial \varphi}{\partial t} + U \frac{\partial \varphi}{\partial x} \right), \tag{17}$$

where $\rho_f$ is the density of fluid.

The following boundary conditions are used to solve equation (16):

$$\varphi = 0 \quad \text{for} \quad x = 0; \qquad \partial \varphi / \partial x = 0 \quad \text{for} \quad x = L_s. \tag{18}$$

The finite-element model of the system of equations (13), (14), (16) is constructed taking into account relations (6) – (12), (15) and (17). The perturbation velocity potential $\varphi$, the basis functions $F_m$, the electric potential difference $\psi$, the electric charge *q,* and the plate membrane displacements *u* and *v* are described using Lagrange bilinear shape functions. The bending displacements *w*, rotation angles $\theta_x$ and $\theta_y$ are approximated by nonconforming cubic Hermite polynomials [33]. Since the plate interacts with the fluid over its entire surface, each node of the

single finite element contains six unknowns: $u$, $v$, $w$, $\theta_x$, $\theta_y$ and $\varphi$. Each $k$-th piezoelectric element has only two unknowns: the potential difference $\psi_k$ and the charge $q_k$. They are common to all its nodes. The discretization of the computational domains of the fluid and the plate is carried out using the spatial 8-node prismatic and flat quadrilateral finite elements, respectively. After implementing the known procedures of the finite element method, we obtain [33, 34]:

$$\mathbf{M}\ddot{\mathbf{u}} + \mathbf{C}\dot{\mathbf{u}} + \mathbf{K}\mathbf{u} + \mathbf{A}\mathbf{u} = \mathbf{r}, \tag{19}$$

$$\mathbf{M} = \begin{bmatrix} \mathbf{M}_f & 0 & 0 & 0 \\ 0 & \mathbf{M}_s & 0 & 0 \\ 0 & 0 & 0 & 0 \\ 0 & 0 & 0 & -\mathbf{L} \end{bmatrix}, \quad \mathbf{C} = \begin{bmatrix} \mathbf{C}_f & \mathbf{C}_{fs} & 0 & 0 \\ 0 & \mathbf{C}_{sf} & 0 & 0 \\ 0 & 0 & 0 & 0 \\ 0 & 0 & 0 & -\mathbf{R} \end{bmatrix},$$

$$\mathbf{K} = \begin{bmatrix} \mathbf{K}_f & 0 & 0 & 0 \\ 0 & \mathbf{K}_s & \mathbf{K}_{sp} & 0 \\ 0 & \mathbf{K}_{ps} & -\mathbf{K}_p & \mathbf{I} \\ 0 & 0 & \mathbf{I} & 0 \end{bmatrix}, \quad \mathbf{A} = \begin{bmatrix} \mathbf{A}_f & \mathbf{A}_{fs} & 0 & 0 \\ 0 & \mathbf{A}_{sf} & 0 & 0 \\ 0 & 0 & 0 & 0 \\ 0 & 0 & 0 & 0 \end{bmatrix},$$

where $\mathbf{u} = \{\boldsymbol{\varphi}, \mathbf{d}, \boldsymbol{\psi}, \mathbf{q}\}^{\mathrm{T}}$, $\mathbf{r} = \{0, \mathbf{f}, 0, 0\}^{\mathrm{T}}$ and typical finite element matrices are determined in a well-known manner:

$$\mathbf{M}_f^e = \int_{V_f} \frac{1}{c^2}\mathbf{F}^{\mathrm{T}}\mathbf{F}\mathrm{d}V, \quad \mathbf{M}_s^e = \int_{S_s} \mathbf{N}^{\mathrm{T}}\mathbf{J}_s\mathbf{N}\mathrm{d}S + \int_{S_{pk}} \mathbf{N}^{\mathrm{T}}\mathbf{J}_{p_k}\mathbf{N}\mathrm{d}S, \quad \mathbf{C}_f^e = \int_{V_f} \frac{2U}{c^2}\frac{\partial \mathbf{F}^{\mathrm{T}}}{\partial x}\mathbf{F}\mathrm{d}V, \tag{20}$$

$$\mathbf{C}_{sf}^e = \int_{S_f} \rho_f \mathbf{N}_w^{\mathrm{T}}\mathbf{F}\mathrm{d}S, \quad \mathbf{C}_{fs}^e = -\int_{S_f} \mathbf{F}^{\mathrm{T}}\mathbf{N}_w\mathrm{d}S, \quad \mathbf{K}_f^e = \int_{V_f} \left(\nabla\mathbf{F}\right)^{\mathrm{T}}\nabla\mathbf{F}\mathrm{d}V, \quad \mathbf{K}_{p_k}^e = C_k,$$

$$\mathbf{K}_{sp}^e = \int_{S_{pk}} \mathbf{B}^{\mathrm{T}}\mathbf{G}\frac{1}{h_{p_k}}\mathrm{d}S, \quad \mathbf{K}_{ps}^e = \int_{S_{pk}} \frac{1}{h_{p_k}}\mathbf{G}^{\mathrm{T}}\mathbf{B}\mathrm{d}S, \quad \mathbf{K}_s^e = \int_{S_s} \mathbf{B}^{\mathrm{T}}\mathbf{S}_s\mathbf{B}\mathrm{d}S + \int_{S_{pk}} \mathbf{B}^{\mathrm{T}}\mathbf{S}_{p_k}\mathbf{B}\mathrm{d}S,$$

$$\mathbf{A}_f^e = -\int_{V_f} \frac{U^2}{c^2}\frac{\partial \mathbf{F}^{\mathrm{T}}}{\partial x}\frac{\partial \mathbf{F}}{\partial x}\mathrm{d}V, \quad \mathbf{A}_{sf}^e = \int_{S_f} \rho_f U\mathbf{N}_w^{\mathrm{T}}\frac{\partial \mathbf{F}}{\partial x}\mathrm{d}S, \quad \mathbf{A}_{fs}^e = -\int_{S_f} U\mathbf{F}^{\mathrm{T}}\frac{\partial \mathbf{N}_w}{\partial x}\mathrm{d}S.$$

Here: $\mathbf{F}$, $\mathbf{N}$, $\mathbf{N}_w$ are the matrices of the shape function for the perturbation velocity potential $\varphi$, the displacement vector of the plate $\mathbf{d}$ and its normal component $w$; $\mathbf{J}$ are the inertia matrices calculated according to expression (15); $\mathbf{B}$ is the gradient matrix, determining the relationship between the deformation and the nodal displacements; $\mathbf{I}$ is the unit matrix.

The formulation of the problem of natural and forced harmonic vibrations of a piecewise homogeneous electroelastic body interacting with a flowing fluid is based on the representation of the solution in the exponential form. In the first case, we use expression (21) and in the second case, we use expression (22):

$$\mathbf{u}(\mathbf{x},t) = \left\{\boldsymbol{\varphi}(\mathbf{x},t), \mathbf{d}(\mathbf{x},t), \boldsymbol{\psi}(\mathbf{x},t), \mathbf{q}(\mathbf{x},t)\right\}^{\mathrm{T}} = \tilde{\mathbf{u}}(\mathbf{x})e^{\mathrm{i}\lambda t}, \tag{21}$$

$$\mathbf{u}(\mathbf{x},t) = \left\{\boldsymbol{\varphi}(\mathbf{x},t), \mathbf{d}(\mathbf{x},t), \boldsymbol{\psi}(\mathbf{x},t), \mathbf{q}(\mathbf{x},t)\right\}^{\mathrm{T}} = \tilde{\mathbf{u}}(\mathbf{x})e^{\mathrm{i}\Omega t}, \quad \mathbf{f}(\mathbf{x},t) = \tilde{\mathbf{f}}(\mathbf{x})e^{\mathrm{i}\Omega t}, \tag{22}$$

where $\tilde{\mathbf{u}}$ is the function depending only on the coordinates $\mathbf{x}$, $\Omega$ is the angular frequency of imposed forces; i is the imaginary unit; $\lambda = \omega + i\gamma$ is the characteristic index, $\omega$ is the natural frequency of vibrations, $\gamma$ is the value, characterizing damping of the system.

Substituting expressions (21) and (22) into the system of equations (19) allows us to obtain:

$$\left(-\lambda^2\mathbf{M} + i\lambda\mathbf{C} + \mathbf{K} + \mathbf{A}\right)\tilde{\mathbf{u}} = 0, \tag{23}$$

$$\left(-\Omega^2\mathbf{M} + i\Omega\mathbf{C} + \mathbf{K} + \mathbf{A}\right)\tilde{\mathbf{u}} = \tilde{\mathbf{r}}. \tag{24}$$

Equation (23) is reduced to the generalized eigenvalue problem (25) for the asymmetric matrices of doubled size [35], which is solved using the implicitly restarted Arnoldi method [36]:

$$\left(\begin{bmatrix} \mathbf{C} & \mathbf{K}+\mathbf{A} \\ -\mathbf{I} & 0 \end{bmatrix} + i\lambda\begin{bmatrix} \mathbf{M} & 0 \\ 0 & \mathbf{I} \end{bmatrix}\right)\begin{Bmatrix} i\lambda\tilde{\mathbf{u}} \\ \tilde{\mathbf{u}} \end{Bmatrix} = 0. \tag{25}$$

The location of the piezoelectric element on the surface of the structure, which will provide its most effective working, is determined numerically from the condition of maximum electromechanical coupling coefficient $K_i$ [2]. It is usually calculated based on $i$-th natural frequencies of vibrations for system with open circuit (hereinafter referred to as "o/c") and closed electrodes (short circuit, hereinafter referred to as "s/c").

Analysis of changes in the complex eigenvalues of the electromechanical system depending on the resistance $R$ and the inductance $L$ of the electric circuit allows us to find their optimal values, providing the maximum rate of natural vibration damping. The condition [37] is used as a criterion:

$$\left|\Delta\lambda_i\right| = \left|\lambda_i - \lambda_{ic}\right| \to \min, \tag{26}$$

where $\lambda_i$ and $\lambda_{ic}$ are the complex eigenvalues corresponding to the damped ($i$-th) mode and mode of electrical circuit connected to the piezoelectric element.

**Verification of the numerical algorithm**

In this section, we demonstrate the performance of the developed finite-element algorithm and the reliability of the solutions to various dynamic problems. Unless otherwise indicated, the calculations were performed using the following parameters: $L_s = 150$ mm, $W_s = 115$ mm, $h_s = 0.5$ mm, $E_s = E_1 = E_2 = 68.5$ GPa, $\nu_s = \nu_{12} = \nu_{21} = 0.3$, $\rho_s = 2714$ kg/m$^3$ (isotropic plate); $L_p = 50$ mm, $W_p = 20$ mm, $h_p = 0.3$ mm, $x_p = 50$ mm, $y_p = 47.5$ mm, $Q_{11} = Q_{22} = 109$ GPa, $Q_{33} = 93$ GPa, $Q_{44} = Q_{55} = Q_{66} = 24$ GPa, $Q_{12} = 61$ GPa, $Q_{13} = Q_{23} = 54$ GPa, $e_{33} = 14.9$ C/m$^2$, $e_{31} = e_{32} = -4.9$ C/m$^2$, $e_{15} = e_{24} = 10.6$ C/m$^2$, $\epsilon_{11} = \epsilon_{22} = 820\epsilon_0$, $\epsilon_{33} = 840\epsilon_0$, $\epsilon_0 = 8.85\times10^{-12}$ F/m; $\rho_p = 7500$ kg/m$^3$ (piezoelectric element); $H = 10$ mm, $\rho_f = 997$ kg/m$^3$, $c = 1500$ m/s (ideal fluid).

*Table 1. Natural vibration frequencies of a plate with piezoelectric element connected to an external RL-circuit*

| $i$ | Plate in vacuum, $R = 2800\ \Omega$, $L = 10.2$ H | | | | Plate interacting with quiescent fluid, $R = 6000\ \Omega$, $L = 61$ H | | | |
|---|---|---|---|---|---|---|---|---|
| | 3D formulation [20] | | Present solution | | 3D formulation [20] | | Present solution | |
| | $\omega_i$ | $\gamma_i$ | $\omega_i$ | $\gamma_i$ | $\omega_i$ | $\gamma_i$ | $\omega_i$ | $\gamma_i$ |
| 1 | **236.033** | **10.907** | **235.494** | **10.951** | 96.970 | 3.870 | 96.769 | 3.895 |
| 2 | 257.511 | 10.883 | 257.870 | 10.837 | **104.708** | **3.939** | **104.837** | **3.913** |

| | | | | | | | | |
|---|---|---|---|---|---|---|---|---|
| 3 | 442.502 | 0.000 | 442.589 | 0.000 | 168.688 | 0.000 | 168.763 | 0.000 |
| 4 | 616.049 | 0.000 | 617.012 | 0.000 | 228.540 | 0.000 | 229.013 | 0.000 |
| 5 | 806.896 | 0.036 | 808.484 | 0.037 | 310.618 | 0.012 | 311.553 | 0.012 |
| 6 | 840.763 | 0.000 | 841.315 | 0.000 | 311.945 | 0.000 | 312.373 | 0.000 |

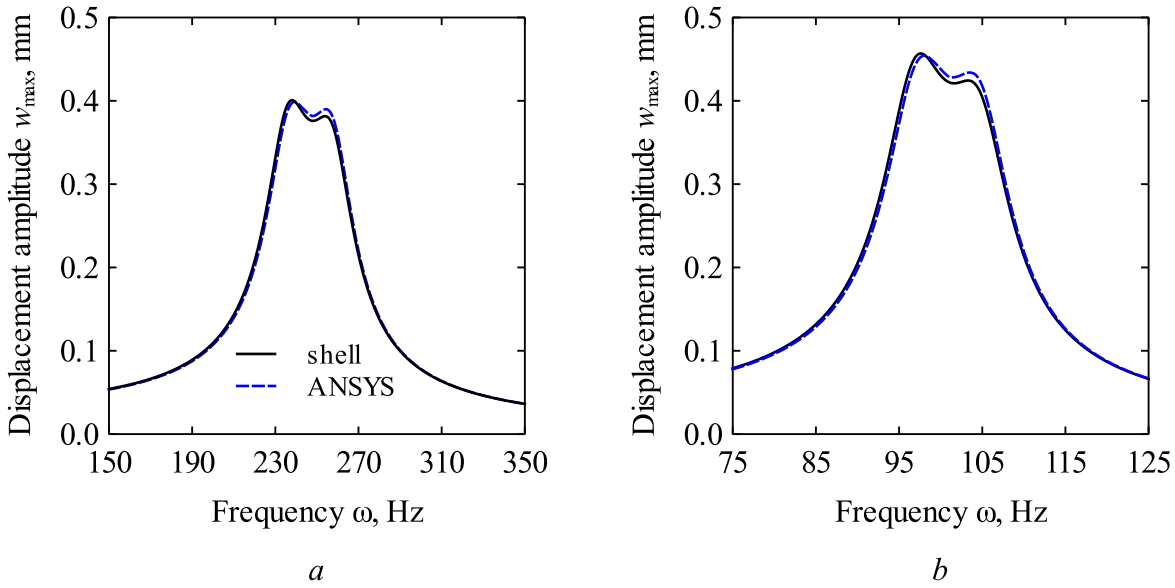


*a* *b*

*Fig. 2. Comparison of frequency response curves of a plate with a piezoelectric element connected to an external RL-circuit: a — plate in vacuum (R = 2800 Ω, L = 10.2 H), b — plate interacting with a quiescent fluid (R = 6000 Ω, L = 61 H)*

We consider the natural vibrations of a rectangular plate rigidly clamped at all edges in vacuum (fluid is absent). A piezoceramic element, whose electroded surfaces are connected to a series *RL*-circuit, is attached to the upper surface of the plate at the point with coordinates $(x_p, y_p)$. Table 1 shows the values of the real and imaginary parts of the complex eigenvalues λ obtained using the above approach *versus* the results of calculations done with the use of three-dimensional equations of the linear theory of piezoelasticity [20]. A similar comparison was made for a plate interacting with a layer of a quiescent fluid of height $H$. The following boundary conditions for the velocity potential φ were used: $\partial\varphi/\partial n = 0$ at the edges $x = 0$, $x = L_s$, $y = 0$, $y = W_s$ and $\varphi = 0$ at $z = H$. In both cases considered, the relative error does not exceed 1% for the vibration frequencies ω and 4% for the damping ratio γ. In this case, the formulation used provides a qualitatively correct description of the appearance of a new natural frequency in the spectrum. It occurs as a result of the formation of a resonant *RLC*-circuit when the piezoelectric element is connected to an external shunt *RL*-circuit. The corresponding mode of vibrations is highlighted in bold type.

The results of solving the problem of forced harmonic vibrations are shown in Fig. 2, which presents the frequency response curves in the vicinity of the first resonance obtained when a uniform pressure of 100 Pa is applied to the plate. All calculation parameters are similar to those considered in the above examples. The dashed line corresponds to the values calculated with the commercial software ANSYS using a three-dimensional formulation. The depicted curves are qualitatively similar, and their maximum quantitative difference does not exceed the value of the relative error of 4%.

**Numerical results**

We consider the plates with two kinds of boundary conditions: rigidly clamped along the perimeter (CCCC) and free only at the edge $x = L_s$ (CCFC). Their distinguishing feature is a significant

difference in the imaginary parts γ of complex eigenvalues obtained at the same fluid flow velocities. This allows us to analyze the performance of the shunt *RL*-circuit in the system with high dissipative characteristics. The calculations were performed for the parameters given at the beginning of the previous section.

The first example demonstrates the possibility of vibration damping for a rectangular plate rigidly clamped at all edges and interacting with the fluid flowing with a velocity of 7 m/s. The parameters of the *RL*-circuit connected to the piezoelectric element ($x_p$ = 54 mm, $y_p$ = 47.5 mm) were determined numerically using condition (26) and are given in Table 2. It also contains the values calculated with the formulas proposed in [2]. Hereinafter, abbreviation "pp" corresponds to the values obtained using the pole placement techniques and abbreviation "tf" – to expressions using the transfer function.

In papers [20, 37], it has been shown that the analytical expressions formulated in [2] do not allow us to obtain the values of inductance and resistance, which would be truly optimal in terms of the rate of vibration damping. Of all the variants considered, only the condition (26) provides the smallest difference between the natural frequencies $\omega_1$ and $\omega_{1c}$ (less than 0.2%). In this case, an increase in the imaginary part $\gamma_1$, relative to the open circuit mode indicates an increase in the damping rate of free vibrations.

*Table 2. Optimal parameters of the external RL-circuit calculated in various ways and complex eigenvalues (Hz) (plate, CCCC, 7 m/s)*

| No. | Solution case | Circuit parameters | | Eigenvalues λ | |
|---|---|---|---|---|---|
| | | *R*, Ω | *L*, H | $\lambda_1$ | $\lambda_{1c}$ |
| 1 | Condition (26) | 324252 | 18781 | 5.5523 + 0.6818 | 5.5605 + 0.6922 |
| 2 | Hagood, pp [2] | 342682 | 19855 | 5.7071 + 0.4438 | 5.2439 + 0.9298 |
| 3 | Hagood, tf [2] | 249497 | 21050 | 5.9372 + 0.3590 | 4.9434 + 0.5843 |
| 4 | Open circuit | $1\times10^{15}$ | $1\times10^{15}$ | 5.5986 + 0.0018 | — |

In the second example, a plate with CCFC boundary conditions is considered. With such kind of boundary condition, the imaginary part of the complex eigenvalues γ, which is responsible for the dissipative characteristics of the system, is several orders of magnitude larger than that in the variant considered above (see rows "Open circuit" in Table 2 and Table 3). In spite of this fact, the connection of a series *RL*-circuit with optimal parameters to the piezoelectric element makes it possible to suppress vibrations even at high modes. The results that confirm this conclusion are given in Table 3. The highest rate of vibration damping is achieved using condition (26).

*Table 3. Optimal parameters of the external RL-circuit calculated in various ways and complex eigenvalues (Hz) (plate, CCFC, 1 m/s)*

| No. | Solution case | Circuit parameters | | Eigenvalues λ | |
|---|---|---|---|---|---|
| | | *R*, Ω | *L*, H | $\lambda_7$ | $\lambda_{7c}$ |
| 1 | Condition (26) | 4296.32 | 13.3203 | 217.209 + 13.253 | 217.283 + 13.313 |
| 2 | Hagood, pp [2] | 3889.40 | 13.1780 | 212.758 + 10.654 | 223.185 + 13.722 |
| 3 | Hagood, tf [2] | 2766.20 | 13.3310 | 208.476 + 8.095 | 226.924 + 9.187 |
| 4 | Open circuit | $1\times10^{15}$ | $1\times10^{15}$ | 217.704 + 1.627 | — |

The frequency response curves, demonstrating the suppression of forced harmonic vibrations, are shown in Fig. 3. They were obtained for the plate under the action of a uniform pressure of 100 Pa. Although in all variants considered, the resonance amplitude decreases by several times.

The best result is attained with the parameter, which are determined in terms of the transfer functions according to the formulas [2] (see curve 3).

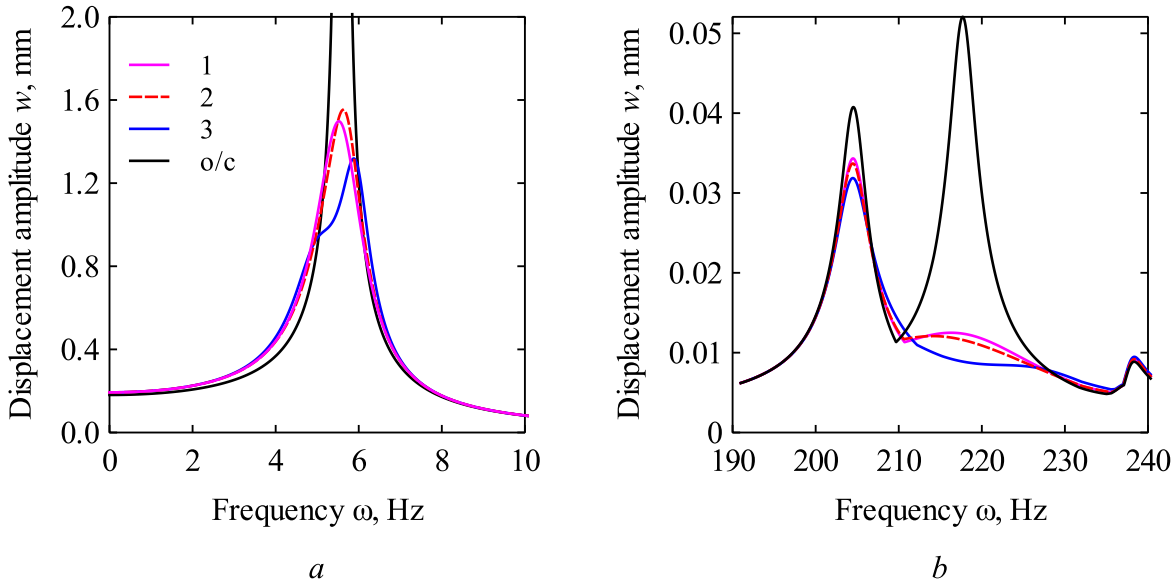


*a* *b*

*Fig. 3. Frequency response curves of a plate with a piezoelectric element connected to an external RL-circuit: a — CCCC (7 m/s), b — CCFC (1 m/s)*

**Conclusion**

A mathematical formulation of the problem and a finite-element algorithm for its numerical implementation have been developed to analyze natural and forced harmonic vibrations of a plate interacting with the flowing fluid and containing the piezoelectric elements connected to external electric circuits.

The dependence of changes in the complex eigenvalues of electromechanical system on the parameters of the electric circuit consisting of a series-connected resistor and inductance has been analyzed. The optimal values of these parameters, providing the most effective suppression of free vibrations in terms of the rate of their decay have been selected. It is shown that compared to the analytical expressions traditionally used for this purpose, the proposed approach makes it possible to obtain higher damping ratios γ.

The frequency response curves, demonstrating a decrease in the amplitude of forced harmonic vibrations at different velocities of the fluid flow, have been obtained. They have been used to compare different ways of calculating the optimal parameters of the *RL*-circuit.

The study was supported by the grant of the Russian Scientific Foundation (project No. 18-71-10054).

**References**

[1] R.L. Forward, Electronic damping of vibrations in optical structures, J. Appl. Optics, 18 (1979) 690–697. https://doi.org/10.1364/AO.18.000690

[2] N.W. Hagood, A.H. von Flotow, Damping of structural vibrations with piezoelectric materials and passive electrical networks, J. Sound Vib., 146 (1991) 243–268. https://doi.org/10.1016/0022-460X(91)90762-9

[3] C.H. Park, D.J. Inman, Enhanced piezoelectric shunt design, Shock Vib., 10 (2003) 127–133. https://doi.org/10.1155/2003/863252

[4] A.J. Fleming, S.O.R. Moheimani, Control orientated synthesis of high-performance piezoelectric shunt impedances for structural vibration control, IEEE Trans. Contr. Syst. Technol., 13 (2005) 98–112. https://doi.org/10.1109/TCST.2004.838547
[5] M. Porfiri, C. Maurini, J.-P. Pouget, Identification of electromechanical modal parameters of linear piezoelectric structures, Smart Mater. Struct., 16 (2007) 323–331. https://doi.org/10.1088/0964-1726/16/2/010
[6] O. Thomas, J. Ducarne, J.-F. Deü, Performance of piezoelectric shunts for vibration reduction, Smart Mater. Struct., 21 (2012) 015008. https://doi.org/10.1088/0964-1726/21/1/015008
[7] P. Soltani, G. Kerschen, G. Tondreau, A. Deraemaeker, Piezoelectric vibration damping using resonant shunt circuits: an exact solution, Smart Mater. Struct., 23 (2014) 125014. https://doi.org/10.1088/0964-1726/23/12/125014
[8] O. Heuss, R. Salloum, D. Mayer, T. Melz, Tuning of a vibration absorber with shunted piezoelectric transducers, Arch. Appl. Mech., 86 (2016) 1715–1732. https://doi.org/10.1007/s00419-014-0972-5
[9] J.F. Toftekær, A. Benjeddou, J. Høgsberg, General numerical implementation of a new piezoelectric shunt tuning method based on the effective electromechanical coupling coefficient, Mech. Adv. Mater. Struct., 27 (2020) 1908–1922. https://doi.org/10.1080/15376494.2018.1549297
[10] J.A.B. Gripp, D.A. Rade, Vibration and noise control using shunted piezoelectric transducers: A review, Mech. Syst. Signal Process., 112 (2018) 359–383. https://doi.org/10.1016/j.ymssp.2018.04.041
[11] A. Presas, Y. Luo, Z. Wang, D. Valentin, M. Egusquiza, A review of PZT patches applications in submerged systems, Sensors, 18 (2018) 2251. https://doi.org/10.3390/s18072251
[12] K. Marakakis, G.K. Tairidis, P. Koutsianitis, G.E. Stavroulakis, Shunt piezoelectric systems for noise and vibration control: A review, Front. Built Environ. 5 (2019) 64. https://doi.org/10.3389/fbuil.2019.00064
[13] A.J. Fleming, S.O.R. Moheimani, Piezoelectric transducers for vibration control and damping, 1st ed., Springer, London, 2006.
[14] J.M. Zhang, W. Chang, V.K. Varadan, V.V. Varadan, Passive underwater acoustic damping using shunted piezoelectric coatings, Smart Mater. Struct., 10 (2001) 414–420. https://doi.org/10.1088/0964-1726/10/2/404
[15] J. Kim, J.-H. Kim, Multimode shunt damping of piezoelectric smart panel for noise reduction, J. Acoust. Soc. Am., 116 (2004) 942–948. https://doi.org/10.1121/1.1768947
[16] J. Kim, Y.-C. Jung, Broadband noise reduction of piezoelectric smart panel featuring negative-capacitive converter shunt circuit, J. Acoust. Soc. Am., 120 (2006) 2017–2025. https://doi.org/10.1121/1.2259791
[17] W. Larbi, J.-F. Deü, R. Ohayon, Finite element formulation of smart piezoelectric composite plates coupled with acoustic fluid. Compos. Struct., 94 (2012) 501–509. https://doi.org/10.1016/j.compstruct.2011.08.010
[18] Y. Sun, Z. Li, A. Huang, Q. Li, Semi-active control of piezoelectric coating's underwater sound absorption by combining design of the shunt impedances, J. Sound Vib., 355 (2015) 19–38. https://doi.org/10.1016/j.jsv.2015.06.036
[19] L. Pernod, B. Lossouarn, J.-A. Astolfi, J.-F. Deü, Vibration damping of marine lifting surfaces with resonant piezoelectric shunts, J. Sound Vib., 496 (2021) 115921. https://doi.org/10.1016/j.jsv.2020.115921

[20] S.V. Lekomtsev, D.A. Oshmarin, N.V. Sevodina, An approach to the analysis of hydroelastic vibrations of electromechanical systems, based on the solution of the non-classical eigenvalue problem, Mech. Adv. Mater. Struct., 28 (2021) 1957–1964. https://doi.org/10.1080/15376494.2020.1716120

[21] M.A. Iurlov, A.O. Kamenskikh, S.V. Lekomtsev, V.P. Matveenko, Passive suppression of resonance vibrations of a plate and parallel plates assembly, interacting with a fluid, Int. J. Struct. Stabil. Dynam., 22 (2022) 2250101. https://doi.org/10.1142/S0219455422501012

[22] J.N. Reddy, Mechanics of laminated composite plates and shells: theory and analysis, 2nd ed., CRC Press, Boca Raton, 2004.

[23] IEEE Standard on Piezoelectricity, ANSI/IEEE Std176-1987, IEEE, New York, 1988. https://doi.org/10.1109/IEEESTD.1988.79638

[24] O. Thomas, J.-F. Deü, J. Ducarne, Vibrations of an elastic structure with shunted piezoelectric patches: efficient finite element formulation and electromechanical coupling coefficients, Int. J. Numer. Meth. Eng. 80 (2009) 235–268. https://doi.org/10.1002/nme.2632

[25] S.H. Moon, S.J. Kim, Active and passive suppressions of nonlinear panel flutter using finite element method, Appl. Math. Model. 39 (2001) 2042–2050. https://doi.org/10.2514/2.1217

[26] G. Yao, F.-M. Li. The stability analysis and active control of a composite laminated open cylindrical shell in subsonic airflow, J. Intel. Mat. Sys. Struct. 25 (2014) 259–270. https://doi.org/10.1177/1045389X13491020

[27] A. Benjeddou, J.-F. Deü, S. Letombe, Free vibrations of simply-supported piezoelectric adaptive plates: an exact sandwich formulation, Thin-Walled Struct. 40 (2002) 573–593. https://doi.org/10.1016/S0263-8231(02)00013-7

[28] G.G. Sheng, X. Wang, Thermoelastic vibration and buckling analysis of functionally graded piezoelectric cylindrical shells, Appl. Math. Model. 34 (2010) 2630–2643. https://doi.org/10.1016/j.apm.2009.11.024

[29] H. Allik, J.R. Hughes, Finite element method for piezoelectric vibration, Int. J. Numer. Meth. Eng. 2 (1970) 151–157. https://doi.org/10.1002/nme.1620020202

[30] M.A. Il'gamov, Vibrations of elastic shells containing liquid and gas, Nauka, Moscow, 1969.

[31] M.P. Païdoussis, Fluid–structure interactions: slender structures and axial flow, Vol. 2, 2nd ed., Elsevier Academic Press, London, 2014.

[32] S.A. Bochkarev, S.V. Lekomtsev, V.P. Matveenko, Hydroelastic stability of a rectangular plate interacting with a layer of ideal flowing fluid, Fluid Dyn. 51 (2016) 821–833. https://doi.org/10.1134/S0015462816060132

[33] O.C. Zienkiewicz, R.L. Taylor, The finite element method. The basis, Vol. 1, 5th ed., Butterworth-Heinemann, Oxford, 2001.

[34] J.N. Reddy, An introduction to nonlinear finite element analysis, 2nd ed., Oxford University Press, London, 2015.

[35] F. Tisseur, K. Meerbergen, The quadratic eigenvalue problem, SIAM Rev., 43 (1988) 235–286. https://doi.org/10.1137/S0036144500381988

[36] R.B. Lehoucq, D.C. Sorensen, Deflation techniques for an implicitly restarted Arnoldi iteration, SIAM J. Matrix Anal. Appl., 17 (1996) 789–821. https://doi.org/10.1137/S0895479895281484

[37] V.P. Matveenko, N.A. Iurlova, D.A. Oshmarin, N.V. Sevodina, M.A. Iurlov, An approach to determination of shunt circuits parameters for damping vibrations, Int. J. Smart Nano Mater., 9 (2018) 135–149. https://doi.org/10.1080/19475411.2018.1461144